

Graph Convolution Networks for Probabilistic Modeling of Driving Acceleration

Jianyu Su,¹ * Peter A. Beling,¹ Rui Guo,² Kyungtae Han,²

¹University of Virginia, ²Toyota Motor North America
{js9wv, pb3a}@virginia.edu, {rui.guo, kyungtae.han}@toyota.com

Abstract

The ability to model and predict ego-vehicle’s surrounding traffic is crucial for autonomous pilots and intelligent driver-assistance systems. Acceleration prediction is important as one of the major components of traffic prediction. This paper proposes novel approaches to the acceleration prediction problem. By representing spatial relationships between vehicles with a graph model, we build a generalized acceleration prediction framework. This paper studies the effectiveness of proposed Graph Convolution Networks, which operate on graphs predicting the acceleration distribution for vehicles driving on highways. We further investigate prediction improvement through integrating of Recurrent Neural Networks to disentangle the temporal complexity inherent in the traffic data. Results from simulation studies using comprehensive performance metrics support the conclusion that our proposed networks outperform state-of-the-art methods in generating realistic trajectories over a prediction horizon.

Autonomous pilots or intelligent driving assistants must be able to predict the future state of traffic in order to warn human drivers about collision risks. The autonomous system in the ego-vehicle should consider not only the ego-vehicle’s interactions with its immediate neighbors, but also hierarchical and chains of interactions that might affect the ego-vehicle’s future state.

Many approaches have been proposed to predict the behavior of vehicles, with most methods falling into the broad categories of regression formulations or classification formulations. While formulating the problem of predicting vehicle behaviors as a classification problem makes it easier to train the model and compare its performance, this approach fails to provide detailed future traffic information for planning the future trajectory. Regression methods, by contrast, are able to infer the future state of traffic, such as vehicle position, velocity and acceleration. In the literature, many of the methods for the regression formulation of traffic prediction employ Recurrent Neural Networks (RNNs). RNNs are widely used to study time-series data. In particular, researchers have been successfully applying Long-Short Term

Memory (LSTM) network to various applications such as speech generation, machine translation, and speech recognition (Hochreiter and Schmidhuber 1997). In this work, we also use an RNN structure as part of our proposed framework.

A principal weakness of existing driving behavior prediction methods is that they use models that require inputs of fixed size and fixed spatial organization, making it difficult to generalize from training sets into practice. In (Morton, Wheeler, and Kochenderfer 2016), for instance, the proposed method uses a leader-follower model that focuses only on the interactions between the ego-vehicle and its leading vehicle. More recently, neighbor models that capture more interactions between ego-vehicle and its surrounding vehicles have been proposed (Alché and de La Fortelle 2017; Lenz et al. 2017). Though these neighbor methods show some success in predicting the ego-vehicle’s future acceleration, they only consider a fixed number of neighbor vehicles. In addition, they need to deal with information padding if one of the pre-defined neighbors is absent.

Graph neural networks (GNNs) are a type of neural network designed for the analysis of graphs (Zhou et al. 2018). Recently, GNNs have been drawing increasing attention from both academia and industry for the flexibility the graph data structure provides and for their convincing performance on various tasks in different domains, such as social science (Hamilton, Ying, and Leskovec 2017; Kipf and Welling 2016), neural science (Fout et al. 2017), and knowledge graphs (Hamaguchi et al. 2017). Motivated by a first-order approximation of spectral convolution on a graph, Graph Convolution Networks (GCNs) are a computationally efficient variant of GNNs that have shown success in achieving fast and scalable classification of nodes in a graph (Kipf and Welling 2016).

In this paper, we propose a flexible driving behavior prediction framework that we call the *Traffic Graph Framework (TGF)*. Combining GNNs and LSTMs, our proposed method is able to capture not only spatial features of various sizes but also temporal features. This framework consists of undirected graphs that represent the interactions between vehicles, a multi-layer graph convolution neural network used to directly encode the graph structure, and a fully-

*Jianyu Su completes this work as an intern in Toyota InfoTech Labs

connected or LSTM mixture density network used to predict future acceleration distributions. The idea of utilizing GCN to predict vehicle’s behavior has been proposed independently and recently by Diehl et al. (Diehl et al. 2019). Note that our method differs from that work in two main ways. First, the model of Diehl et al. considers only up to 8 neighbors, which might result in ignoring important information about the state of traffic around ego-vehicles. In contrast, our framework does not place a hard constraint to the number of neighbors. Second, Diehl et al. do not consider RNN structure, which is able to memorize the past states of a vehicle. We believe that, in the task of driving, information of ego-vehicle’s past states affects future actions. Hence, we include RNN structure in our framework and analyze the performance of GCNs with and without RNNs.

Finally, experiments are designed to analyze the effectiveness of the proposed GCNs and RNN architecture, respectively. A simulation is built based on the NGSIM I-80 dataset, which contains vehicle trajectories of more than 2000 individual drivers, to mimic the real-world traffic (Colyar and Halkias 2006). In the simulation, ego-vehicles’ traffic states are propagated based on models’ predictions. Models are evaluated by comprehensive metrics to measure the discrepancy between their predicted trajectories and the ground truth. Our results shows that including the proposed GCNs and RNN structure improves model’s prediction quality.

Our principal contributions are two-fold:

- We propose a graph structure to denote vehicle’s spatial relationships in a dynamic traffic environment.
- We introduce new variants of GCN layer-wise propagation rule in the context of traffic modeling and we propose a new acceleration prediction framework combining GCNs and LSTM. We successfully applied our framework to a real-world simulation. The resulting systems outperform others from the literature on the task of acceleration prediction.

Related Work

The task of modeling driving behavior consists of modeling car-following behavior and lane-changing behavior. In our work, we focus on augmenting the car-following model.

Car-following models capture the interaction between the ego-vehicle and the vehicles directly adjacent on the microscopic level of the traffic. Based on number of interactions captured, models can be categorized as being either single-lane or multiple-lane.

A single-lane model focuses on the interactions between vehicles in a single lane. This model considers up to two kinds of interactions: namely, the ego-vehicle with its leading vehicle, and the ego-vehicle with its following vehicle. Many traditional fixed-form models fall into this category, including the Gazis-Herman Rothery model (Chandler, Herman, and Montroll 1958), the collision avoidance model (Kometani 1959), linear models (Helly 1959), psycho-physical models (Michaels 1963), and fuzzy logic-based models (Kikuchi and Chakraborty 1992).

Some recent general driving models have moved away from making assumptions about drivers. Lefvre et al. compare the performance of feed-forward mixture density network against traditional baselines (Lefèvre et al. 2014). Their empirical tests suggest that the proposed method is able to achieve performance comparable to the baselines. Morton et al. study the effectiveness of LSTM in predicting driving behavior on highways. They reveal that the LSTM’s ability to remember historic states of the ego-vehicle appears to be key to achieving state-of-art performance (Morton, Wheeler, and Kochenderfer 2016).

More recently, multiple-lane models that consider more interactions, coupled with neural networks, have been introduced in the literature. Kim et al. propose a framework based on LSTM to predict vehicle’s future position over the occupancy grid. (Kim et al. 2017). Altche et al. use a LSTM that predicts traffic using as input state information on the ego-vehicle states and up to 9 of its neighbors. The model is trained and evaluated on the NGSIM 101 dataset which collected trajectories from more than 6000 individual drivers (Altché and de La Fortelle 2017).

The rest of this paper is organized as follows: In Methodology section, we introduce our framework and our proposed GCN variants. In Experiment section, we present the training procedure and simulation results for all models. In Discussion section, we elaborate on our findings about GCNs and LSTM in the experiment. Finally, the final section concludes the study.

Methodology

This section describes the construction of traffic graphs and our proposed graph convolution network variants.

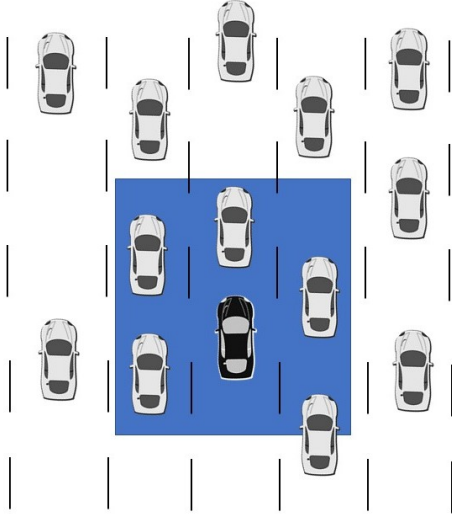
Traffic Graph and Features

To leverage the spatial relationships and interactions between vehicles on the highway, we use an undirected graph $G = (E, V)$ with N nodes $v_i \in V$, edges $(v_i, v_j) \in E$, an adjacency matrix $A \in \mathbb{R}^{N \times N}$, a degree matrix with $D_{ii} = \sum_j A_{ij}$, and a nodes feature information matrix $X \in \mathbb{R}^{N \times F}$ to model the interactions between vehicles. As shown in figure 1, for a vehicle pair (v_i, v_j) where $v_i \in V$ and $v_j \in V$, the edge (v_i, v_j) is connected if and only if:

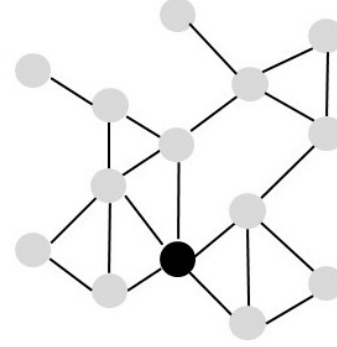
- vehicle v_j and v_i appear at the same frame; and
- vehicle v_j is less than one lane away from vehicle v_i at the current frame(vehicle v_j should be on the same lane with vehicle v_i or on vehicle i ’s left, right lanes); and
- the absolute value difference of vehicle v_j ’s y -coordinate and vehicle v_i ’s y -coordinate is less than the designated value τ at the current frame.

Note that there is no fixed limit on the number of neighbors; all vehicles within a ego-vehicle’s designated distance τ are its neighbor vehicles.

In this work, we adopt the features used in (Lenz et al. 2017). For a vehicle node in the graph at frame t , its feature vector includes the following elements: vehicle lane l_t



(a) An ego-vehicle only considers vehicles within 1 lanes away as potential neighbor vehicles. A potential neighbor vehicle will be deemed as ego-vehicle’s neighbor if and only if the absolute value of their headway distance is smaller than τ



(b) A graph is constructed by connecting every vehicle with their neighbor vehicles

Figure 1: Mapping from real world traffic to traffic graph

(one-hot-encoded), vehicle class c (one-hot-encoded), vehicle velocity v_t , vehicle acceleration a_t , relative distance from 3 nearest front neighbor vehicles $\{d_{f_1}, d_{f_2}, d_{f_3}\}$ (pad τ if the number of front neighbors is smaller than 3), and negative relative distance from 3 nearest rear neighbor vehicles $\{-d_{r_1}, -d_{r_2}, -d_{r_3}\}$ (pad $-\tau$ if the number of rear neighbors is less than 3).

Graph Convolution Network

GCN takes input as a graph G and output nodes encodings. We consider the propagation rule originally introduced in (Kipf and Welling 2016) as our base model:

$$H^{l+1} = \sigma(\hat{D}^{-\frac{1}{2}} \hat{A} \hat{D}^{-\frac{1}{2}} H^l W^l), \quad (1)$$

where $\hat{A} = A + I_N$ is the summation of the undirected graph G ’s adjacency matrix with binary entries A and self-connection $I_N \in \mathbb{R}^N$, $I_N \in \mathbb{R}^N$ is a identity matrix, D is a degree matrix with $D_{ii} = \sum_j A_{ij}$, $W^l \in \mathbb{R}^{N \times C^l}$ is a matrix of trainable weights at depth l , σ is an activation function, and H^l is the encoding of all nodes in the graph at depth l ($H^0 = X$).

This layer-wise propagation rule can be rewritten in the following vector form:

$$h_{v_i}^{l+1} = \sigma\left(\sum_j \frac{h_{v_j}^l}{c_{ij}} W^l + \frac{h_{v_i}^l}{c_{ii}} W^l\right). \quad (2)$$

Here, j indexes neighboring nodes of v_i , normalization factor $\frac{1}{c_{ij}}$ is an entry located at the i th row, j th column of $\hat{D}^{-\frac{1}{2}} \hat{A} \hat{D}^{-\frac{1}{2}}$.

The propagation rule represented by Equation 1 is a first-order approximation of spectral convolution on a graph. It provides two advantages when used to analyze graphs: first, it enables to aggregate l^{th} order neighborhood of a central node during the encoding process; second, it prevents us from prohibitively expensive eigendecomposition of the graph Laplacian compared with spectral convolution models (Kipf and Welling 2016). Those properties offer us a computational efficient approach to learn the interactions between vehicles that are not directly connected in the graph.

Ego-discriminated GCN (EGCN): During the implementation of the base model, we find that self-connection affects the performance of the system, an observation that leads to our adaptation of the base model. Self-connection was used to alleviate the problem of vanishing/exploding gradients in GCNs (Kipf and Welling 2016). However, this method applies the same weight W^l to both the central node and its surrounding nodes. In our experiments, we find it is beneficial to remove the self-connection and apply different layer weights to discriminate the central node from its surrounding node. This leaves us with the ego-discriminated propagation rule, which can be represented as follows:

$$H^{l+1} = \sigma\left(AGG(D^{-\frac{1}{2}} A D^{-\frac{1}{2}} H^l W^l, I_N H^l B^l)\right), \quad (3)$$

where $I_N \in \mathbb{R}^N$ is an identity matrix, $B^l \in \mathbb{R}^{N \times C^l}$ is trainable weights at depth l for central nodes and $AGG(M_1, M_2)$ is a matrix operation function to aggregate two matrices of the same shape. To avoid introducing additional parameters,

we only consider matrix addition and concatenation in this work:

$$AGG(M_1, M_2) = \begin{cases} M_1 + M_2, & \text{addition} \\ [M_1, M_2], & \text{concatenation} \end{cases} \quad (4)$$

The corresponding vector form is given in the following expression:

$$h_{v_i}^{l+1} = \sigma \left(AGG \left(\sum_j \frac{h_{v_j}^l}{c_{ij}} W^l + \frac{h_{v_i}^l}{c_{ii}} B^l \right) \right). \quad (5)$$

Distance-Aware Graph Convolution Network

Distance-Aware Graph Convolution Network (DGCN): For the models mentioned in the previous section, their adjacency matrices \hat{A} and A only denote whether a pair of vehicles is close or not, but they do not describe the degree of closeness. Based on our empirical driving experience—the closer our neighbor vehicle is, the more attention we will pay to it—we use absolute inverse relative distances as entries for our adjacency matrix \tilde{A} to differentiate the degree of closeness between vehicles. Therefore, we introduce the following distance-aware layer-wise propagation rule in our multi-layer GCN:

$$H^{l+1} = \sigma \left(AGG \left(\tilde{D}^{-\frac{1}{2}} \tilde{A} \tilde{D}^{-\frac{1}{2}} H^l W^l, I_N H^l B^l \right) \right). \quad (6)$$

Here, \tilde{A} is an adjacency matrix with $\tilde{A}_{ij} = \frac{1}{|y_{v_i} - y_{v_j}|}$ where y_i represents vehicle v_i 's y -coordinate. \tilde{D} is a degree matrix with $\tilde{D}_{ii} = \sum_j \tilde{A}_{ij}$. In this propagation rule, \tilde{A} 's entries denote the degree of closeness between vehicles. To stabilize gradients during training, we discretize the degree of closeness into three levels: 1, 2, and 3, which represent far away, medium close and very close, respectively. Equation 6 can also be rewritten in the following vector form:

$$h_{v_i}^{l+1} = \sigma \left(AGG \left(\sum_j \frac{h_{v_j}^l}{\tilde{c}_{ij}} W^l + h_{v_i}^l B^l \right) \right), \quad (7)$$

where \tilde{c}_{ij} is an entry located at i th row and j th column of $\tilde{D}^{-\frac{1}{2}} \tilde{A} \tilde{D}^{-\frac{1}{2}}$.

Gaussian Mixture Model

In this work, we aim to predict human driver's acceleration distribution given the current traffic state. Hence the output of our network model is Gaussian mixture model (GMM) parameters that characterize the future acceleration distribution (Bishop 1994). For a K -component GMM, the probability of the predicted acceleration follows this equation:

$$p(a) = \sum_{i=1}^K w_i \mathcal{N}(a | \mu_i, \sigma_i^2), \quad (8)$$

where w_i , μ_i , and σ_i are the weight, mean, standard deviation of the i th mixture component respectively. This approach has been successfully applied in speech recognition and other fields (Robinson, Hochberg, and Renals 1996).

Experiment

Dataset

The NGSIM I-80 dataset contains detailed vehicle trajectory data collected using synchronized digital video cameras on eastbound I-80 in Emeryville, CA. This dataset provides precise positions, velocities and other vehicle information over three 15 minute periods at 10 Hz. The study area covers approximately 500 meters in length and consists of six free-way lanes, including a high-occupancy lane and an onramp. We use the NGSIM I-80 reconstructed dataset, which contains vehicles' precise position, velocity, acceleration from 4:00 p.m. to 4:15 p.m., because it corrects errors such as extreme acceleration, and inconsistent vehicle IDs (Montanino and Punzo 2013) (Montanino and Punzo 2015). We split the data into training sets and testing sets by a ratio of 4 to 1.

Data Preparation

Both training set and testing set are divided into 12-second segments (120 frames). The first 2-second segments (20 frames) are used to initialize the internal state of LSTM networks. Since the aim of the research is to predict driving acceleration using GCNs, we need to prepare traffic graphs from the raw data.

Baselines

Our proposed models are compared with two non-GCN neural networks.

Fully-connected (FC): This model shares the same configuration and input features as the GCN model. This model is a baseline to fully-connected GCN models.

LSTM: This model's configuration and input features are the same with GCN-LSTM model. This model is used as a baseline to GCN models with LSTM structure.

Table 1 summarizes the output size of each layer in models used in this work.

Implementation

All models are trained to output predicted parameters for distributions over future acceleration values. Note that every model in this work shares the same hyperparameters because we aim to compare the effectiveness of GCN and LSTM on improving model performance in the task of driver behavior prediction. We set $\tau = 20$ feet, empirically.

Model structures are shown in Table 1. Each model consists of 3 hidden layers and a 30-component Gaussian mixture output layer. Layer 1 applies Relu activation while other layers do not use any activation. Layer 1 and layer 2 are followed by batch normalization. Batch normalization is a mechanism to address the problem of *internal covariate shift*. It has been reported that adding batch normalization to state-of-the-art image classification networks yields higher classification accuracy compared with the original networks (Ioffe and Szegedy 2015). The performance of our models is also found to improve when batch normalization is applied.

All models are trained for 5 epochs. During training, the models are optimized by adam-optimizer with a learning rate of 1×10^{-3} (Kingma and Ba 2014). A dropout of 10 percent is applied to help prevent overfitting. Gradient norm

clipping is also used to deal with gradient vanishing and gradient explosion (Pascanu, Mikolov, and Bengio 2013). All networks are implemented in tensorflow (Abadi et al. 2016) based on Kpif’s GCN package (Kipf and Welling 2016).

Note that we consider two matrix aggregation methods as mentioned in Equation 4. We conducted a hyperparameter sweep to select aggregation method. Final model configurations are listed in Table 1.

Evaluation

Once trained, each model is used to generate simulated trajectories. For every trajectory in the test set, the first 2-second segments (20 frames) of true data are used to initialize LSTM’s internal state. In the following 10 seconds, ego-vehicle’s velocity and position can be updated by assuming the following equations:

$$\begin{aligned} v(t + \delta t) &= v(t) + a(t + \delta t) \times \delta \\ y(t + \delta t) &= y(t) + v(t + \delta t) \times \delta, \end{aligned} \quad (9)$$

where v is ego-vehicle’s velocity, y is ego-vehicle’s y coordinate and a is vehicle’s acceleration. The graph and node features are updated by propagate other vehicles’ true trajectory data and ego-vehicle’s simulated trajectory. Following the practice in (Morton, Wheeler, and Kochenderfer 2016), we evaluate the quality of simulated trajectories by the following metrics:

- **Root Mean Squared Error (RMSE):** We use root mean squared error to evaluate the discrepancy of speed values between simulated trajectories and true trajectories at designated horizons for a given ego-vehicle:

$$RMSE_{velocity} = \sqrt{\frac{1}{mn} \sum_{i=1}^m \sum_{j=1}^n (v_H^i - \hat{v}_H^{i,j})^2}, \quad (10)$$

where m is the number true trajectory, $n = 20$ is the number of simulated trajectory per true trajectory, v_H^i is the velocity of i th true trajectory at horizon H , $\hat{v}_H^{i,j}$ is the value in j th simulated trajectory at time horizon H . Similarly, we also use root mean squared error to evaluate the displacement in y coordinate at 10 second horizon between simulated trajectories and true trajectories:

$$RMSE_Y = \sqrt{\frac{1}{mn} \sum_{i=1}^m \sum_{j=1}^n (y^i - \hat{y}^{i,j})^2}, \quad (11)$$

where y^i is the y coordinate of i th true trajectory at 10 second, $\hat{y}^{i,j}$ is the simulated y coordinate value for sample j in the i th trajectory at 10 second horizon.

Figure 2 shows the velocity RMSE for the top 6 models over prediction horizons between 1 and 10 seconds. Models with original GCN (Kipf and Welling 2016) are not included because of their bad performance in generating predicted trajectories. In general, the velocity RMSE accumulates over the time horizon. Our adapted GCN models outperform non-GCN models. For non-GCN models, LSTM outperforms the fully-connected model because

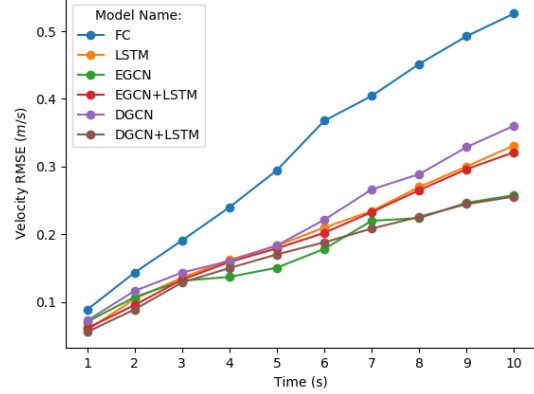


Figure 2: RMSE results for all models

LSTM is able to access past information. For GCN models, EGCN model and DGCN with LSTM outperform other GCN models.

The Y-coordinate RMSE column in Table 2 denotes the displacement in Y-coordinate between simulated trajectories and their corresponding true trajectories. EGCN model outperforms other models. Velocity RMSE at 10 second horizon reveals the discrepancy of speed between simulated trajectories and the ground truth. DGCN with LSTM outperforms other models in this metric.

- **Negative Headway Distance Occurrence:** This metric is used to evaluate models’ robustness. It records the occurrences of unrealistic states led by models’ poor decision making. Two types of negative headway distances are considered: (1) ego-vehicle’s negative headway distance representing collisions with the front vehicle; and (2) following vehicle’s negative headway distance denoting collisions between the ego-and its following vehicle. A robust model will have minimal negative headway distance occurrence.

Table 3 shows the number of negative headway occurrences over number of simulated trajectories for all models. Consistent with RMSE analysis, the results from Table 3 demonstrates that original GCN models often produce poor acceleration predictions which lead to unrealistic states. EGCN model and DGCN with LSTM model are robust because there are no unrealistic states occurring in their simulated trajectories.

- **Jerk Sign Inversions:** We use the number of jerk sign inversions per trajectory to evaluate the similarity between the smoothness of the true and simulated trajectories. This metric is used to quantify oscillations in model’s acceleration predictions.

Simulated trajectories of most of models have slightly higher jerk sign inversions than the true trajectories while the LSTM baseline model is not able to generate smooth trajectories.

Figure 3 shows the sample simulated trajectories by mod-

Table 1: Model Configuration

Model	layer 1	layer 2	layer 3	LSTM	AGG type	clip norm	adjacency type
Fully-connected	128	256	90	no	/	5	/
GCN base	128	256	90	no	/	5	binary
EGCN	128	256	90	no	add	5	binary
DGCN	128	256	90	no	concat	5	inverse distance
LSTM	128	256	90	yes	/	5	/
GCN with LSTM	128	256	90	yes	/	5	binary
EGCN with LSTM	128	256	90	yes	add	5	binary
DGCN with LSTM	128	256	90	yes	add	5	inverse distance

Table 2: RMSE Analysis

Model	Y RMSE @ 10 s (m)	Velocity RMSE @ 10 s (m/s)
Fully-connected (FC)	2.89	0.526
GCN base	3.52	0.622
EGCN	1.40	0.258
DGCN	1.91	0.360
LSTM	1.61	0.331
GCN with LSTM	3.40	0.653
EGCN with LSTM	1.86	0.321
DGCN with LSTM	1.63	0.256

Table 3: Jerk Sign Inversions Per Trajectory

Model	Jerk Sign Inversions	Negative Headway Occurrence Rate
Fully-connected (FC)	7.5	0.08
GCN base	7.5	0.17
EGCN	7.5	0
DGCN	7.3	0.03
LSTM	13.7	0.02
GCN with LSTM	6.7	0.17
EGCN with LSTM	9.5	0.01
DGCN with LSTM	7.3	0
True trajectory	6.3	/

els including adapted GCN models and non-GCN models. It can be seen that non-GCN models predict poorly if the ground truth trajectory includes a long period of acceleration values that are very close to zero while GCN models is able to generate smooth trajectories close to the ground truth. In addition, non-GCN models are prone to predict extreme acceleration values, which is compensated by oscillation of acceleration values.

Discussion

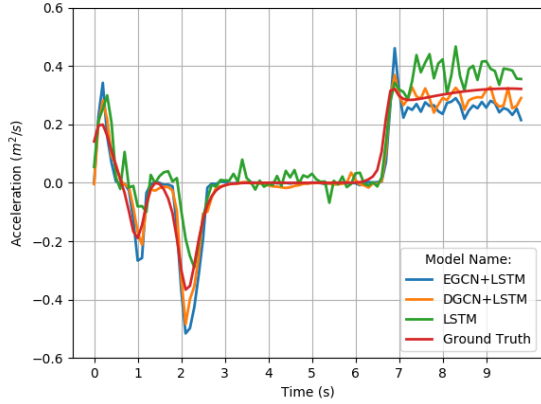
Our experiments are designed to answer the following research questions:

- Does GCN improve model performance and is our adaptations to GCN beneficial?
- Does including LSTM increase prediction quality?

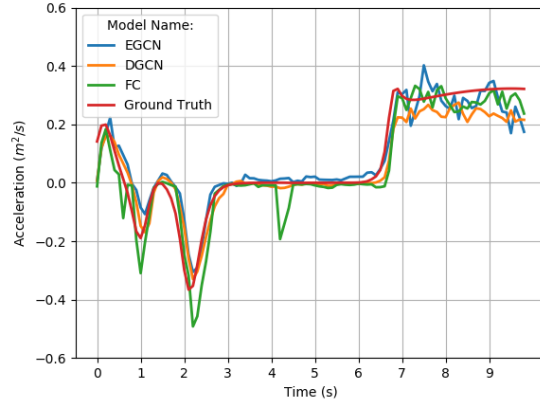
First, we discover that we improve GCN’s performance when we delete self-connections and apply different weights to the central nodes and their surrounding nodes. For GCN base model, we reduced velocity RMSE by 58.5% at 10 sec-

onds horizon and negative headway occurrence by 17% during simulation. For GCN with LSTM model, we reduced its 10 seconds horizon velocity RMSE by 50.8% and negative headway occurrence by 15%.

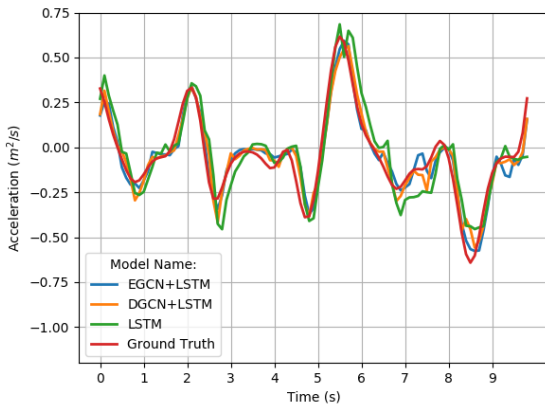
Second, our experiments demonstrated that GCNs improve model performance. GCN models are able to generate smooth and robust trajectories close to the ground truth. For both LSTM and fully-connected models, the non-GCN baseline model is outperformed by its GCN counterparts, in general. Note that, during the experiments, our GCN models and non-GCN models share the same number of hidden layers and the same number of neurons in each hidden layer. Compared with non-GCN fully-connected model, our EGCN model reduced the negative headway occurrence rate from 0.08 to 0, 10 seconds horizon velocity RMSE by 59.6%. Compared with non-GCN LSTM, our DGCN with LSTM reduced the negative headway occurrence rate from 0.02 to 0, jerk sign inversions from 13.7 to 7.3 and 10 seconds horizon velocity RMSE by 22.7%. This trend can also be observed in Figure 3. The multi-layer GCN’s ability to



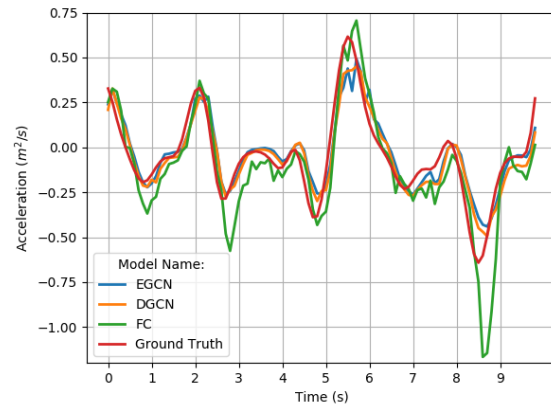
(a) LSTM models



(b) Fully-connected models



(c) LSTM models



(d) Fully-connected models

Figure 3: Simulated Trajectories For All Models

capture multitudes of interactions between vehicles hierarchically improves model’s prediction quality in terms of our evaluation metrics.

In general, we find that adding LSTM structure improves model prediction quality. Among all models, the best model is DGCN with LSTM. During simulation, this model is able to generate robust and smooth driving trajectories with 0 negative headway, 7.3 jerk sign inversions and 0.256 for 10-second horizon velocity RMSE.

Conclusion

In this article, we proposed the use of graphs defined by the spatial relationships between vehicles, to model traffic. We further build GCN models, operating on graphs, to predict future acceleration distributions. We proposed two GCN models adapted from the state-of-art GCN and studied the effectiveness of integrating LSTM architectures in our prediction models. Our resulting frameworks outperform others on the task of acceleration prediction.

While our work has been shown to improve prediction performance, much work remains to be done: This work only considers acceleration prediction, it can be extended to predictions in two dimensions. At the same time, it will be interesting to evaluate different graph construction strategies, such as strategies that include multiple layers of relationships.

References

- [Abadi et al. 2016] Abadi, M.; Barham, P.; Chen, J.; Chen, Z.; Davis, A.; Dean, J.; Devin, M.; Ghemawat, S.; Irving, G.; Isard, M.; et al. 2016. Tensorflow: A system for large-scale machine learning. In *12th USENIX Symposium on Operating Systems Design and Implementation (OSDI 16)*, 265–283.
- [Althé and de La Fortelle 2017] Althé, F., and de La Fortelle, A. 2017. An lstm network for highway trajectory prediction. In *2017 IEEE 20th International*

- Conference on Intelligent Transportation Systems (ITSC)*, 353–359. IEEE.
- [Bishop 1994] Bishop, C. M. 1994. Mixture density networks.
- [Chandler, Herman, and Montroll 1958] Chandler, R. E.; Herman, R.; and Montroll, E. W. 1958. Traffic dynamics: studies in car following. *Operations research* 6(2):165–184.
- [Colyar and Halkias 2006] Colyar, J., and Halkias, J. 2006. Us highway 80 dataset, federal highway administration (FHWA), vol. *Tech, no. Rep.*
- [Diehl et al. 2019] Diehl, F.; Brunner, T.; Le, M. T.; and Knoll, A. 2019. Graph neural networks for modelling traffic participant interaction. *arXiv preprint arXiv:1903.01254*.
- [Fout et al. 2017] Fout, A.; Byrd, J.; Shariat, B.; and Ben-Hur, A. 2017. Protein interface prediction using graph convolutional networks. In *Advances in Neural Information Processing Systems*, 6530–6539.
- [Hamaguchi et al. 2017] Hamaguchi, T.; Oiwa, H.; Shimbo, M.; and Matsumoto, Y. 2017. Knowledge transfer for out-of-knowledge-base entities: A graph neural network approach. *arXiv preprint arXiv:1706.05674*.
- [Hamilton, Ying, and Leskovec 2017] Hamilton, W.; Ying, Z.; and Leskovec, J. 2017. Inductive representation learning on large graphs. In *Advances in Neural Information Processing Systems*, 1024–1034.
- [Helly 1959] Helly, W. 1959. Simulation of bottlenecks in single-lane traffic flow.
- [Hochreiter and Schmidhuber 1997] Hochreiter, S., and Schmidhuber, J. 1997. Long short-term memory. *Neural computation* 9(8):1735–1780.
- [Ioffe and Szegedy 2015] Ioffe, S., and Szegedy, C. 2015. Batch normalization: Accelerating deep network training by reducing internal covariate shift. *arXiv preprint arXiv:1502.03167*.
- [Kikuchi and Chakroborty 1992] Kikuchi, S., and Chakroborty, P. 1992. Car-following model based on fuzzy inference system. *Transportation Research Record* 82–82.
- [Kim et al. 2017] Kim, B.; Kang, C. M.; Kim, J.; Lee, S. H.; Chung, C. C.; and Choi, J. W. 2017. Probabilistic vehicle trajectory prediction over occupancy grid map via recurrent neural network. In *2017 IEEE 20th International Conference on Intelligent Transportation Systems (ITSC)*, 399–404. IEEE.
- [Kingma and Ba 2014] Kingma, D. P., and Ba, J. 2014. Adam: A method for stochastic optimization. *arXiv preprint arXiv:1412.6980*.
- [Kipf and Welling 2016] Kipf, T. N., and Welling, M. 2016. Semi-supervised classification with graph convolutional networks. *arXiv preprint arXiv:1609.02907*.
- [Kometani 1959] Kometani, E. 1959. Dynamic behavior of traffic with a nonlinear spacing-speed relationship. *Theory of Traffic Flow (Proc. of Sym. on TTF (GM))* 105–119.
- [Lefèvre et al. 2014] Lefèvre, S.; Sun, C.; Bajcsy, R.; and Laugier, C. 2014. Comparison of parametric and non-parametric approaches for vehicle speed prediction. In *2014 American Control Conference*, 3494–3499. IEEE.
- [Lenz et al. 2017] Lenz, D.; Diehl, F.; Le, M. T.; and Knoll, A. 2017. Deep neural networks for markovian interactive scene prediction in highway scenarios. In *2017 IEEE Intelligent Vehicles Symposium (IV)*, 685–692. IEEE.
- [Michaels 1963] Michaels, R. 1963. Perceptual factors in car-following. *Proc. of 2nd ISTTF (London)* 44–59.
- [Montanino and Punzo 2013] Montanino, M., and Punzo, V. 2013. Making ngsim data usable for studies on traffic flow theory: Multistep method for vehicle trajectory reconstruction. *Transportation Research Record* 2390(1):99–111.
- [Montanino and Punzo 2015] Montanino, M., and Punzo, V. 2015. Trajectory data reconstruction and simulation-based validation against macroscopic traffic patterns. *Transportation Research Part B: Methodological* 80:82–106.
- [Morton, Wheeler, and Kochenderfer 2016] Morton, J.; Wheeler, T. A.; and Kochenderfer, M. J. 2016. Analysis of recurrent neural networks for probabilistic modeling of driver behavior. *IEEE Transactions on Intelligent Transportation Systems* 18(5):1289–1298.
- [Pascanu, Mikolov, and Bengio 2013] Pascanu, R.; Mikolov, T.; and Bengio, Y. 2013. On the difficulty of training recurrent neural networks. In *International conference on machine learning*, 1310–1318.
- [Robinson, Hochberg, and Renals 1996] Robinson, T.; Hochberg, M.; and Renals, S. 1996. The use of recurrent neural networks in continuous speech recognition. In *Automatic speech and speaker recognition*. Springer. 233–258.
- [Zhou et al. 2018] Zhou, J.; Cui, G.; Zhang, Z.; Yang, C.; Liu, Z.; and Sun, M. 2018. Graph neural networks: A review of methods and applications. *arXiv preprint arXiv:1812.08434*.